

Cell-Free MIMO in 6G NTN with AI-predicted CSI

Bruno De Filippo*, Riccardo Campana*, Alessandro Guidotti[†], Carla Amatetti*, Alessandro Vanelli-Coralli*

*Dept. of Electrical, Electronic, and Information Engineering (DEI), Univ. of Bologna, Bologna, Italy

[†]National Inter-University Consortium for Telecommunications (CNIT), Italy

{bruno.defilippo, riccardo.campana7, a.guidotti, carla.amatetti2, alessandro.vanelli}@unibo.it

Abstract—Non-Terrestrial Networks (NTNs) in 6G are expected to integrate the Terrestrial Networks (TNs) coverage and provide connectivity to a multitude of User Terminals (UTs). In order to cope with the traffic demand, NTN can employ cell-free MIMO with full frequency reuse schemes to maximize the spectral efficiency of the system. However, such technique can be strongly affected by channel aging, impacting their application to Low Earth Orbit (LEO)-based NTNs. Aiming at counteracting this effect, we present in this paper a lightweight Artificial Intelligence (AI) model for Channel State Information (CSI) prediction. To predict the propagation channel, the proposed algorithm learns its temporal statistics, *e.g.*, the Line-of-Sight (LoS) shadowing correlation, from data. The model then applies the corrections to the feedback CSI, minimizing the difference with respect to the propagation channel encountered at transmission time. System-level analyses on a LEO-based CF-MIMO system report an improvement of the per-user capacity by up to 15% and a reduction of the outage probability when predicted CSI are used instead of aged channel coefficients.

Index Terms—Cell-free MIMO, Channel Prediction, Artificial Intelligence, Non-Terrestrial Networks

I. INTRODUCTION

Non-terrestrial networks (NTNs) have recently seen a steep growth in interest from both the scientific research and the industrial side. On the one hand, advanced interconnected satellite constellations with federated multiple input multiple output (MIMO) capabilities are being theorized [1]. On the other hand, unmodified handheld user terminals (UTs) have been proven able to close the link budget with low Earth orbit (LEO) satellites using third generation partnership project (3GPP)-compliant communication standards [2]. Thanks to digital beamforming, NTN systems can dynamically generate beams pointing towards a service area or, more specifically, towards single users in a cell-free (CF) fashion with full frequency reuse. In the NTN context, CF-MIMO systems may be implemented with multiple satellites, in a federated fashion, or with a single satellite, moving from the traditional fixed beam lattice to a user-centric coverage. Such technique has been demonstrated successful in improving the spectral efficiency in NTNs, resulting in an increased data rate experienced by the users. With the next generation 3GPP standard, 6G, foreseeing the integration of NTNs and terrestrial networks, CF-MIMO may be employed to enable higher spectral efficiency in NTNs, aiming at coping with the large expected traffic demand [3]. However, CF-MIMO systems typically rely on a downlink channel state information (CSI) feedback from the UTs to the ground station where digital beamforming coefficients are computed. Due to the

intrinsic propagation distance that characterizes NTNs, the link is subject to strong delays, resulting in the CSI being partially outdated once they are received by the ground station. This effect, known as "channel aging", affects system performance, as the feedback CSI accuracy with respect to the propagation channel at transmission time is crucial to generate optimal CF beams. To counteract this, several artificial intelligence (AI) algorithms have been investigated. Such methods can be employed to extract the propagation channel statistics through a learning process and apply the gained knowledge to improve the feedback CSI, aiming at matching the future channel conditions. The authors in [4] trained a long short term memory (LSTM) model to process a time series of CSI and output consecutive CSI predictions. The work took into account the deterministic line-of-sight (LoS) component of the CSI, as well as random effects due to multiple secondary paths in the non-LoS (NLoS) component. In [5], a convolutional neural network (CNN) was implemented to transform uplink CSI into downlink CSI, aiming at removing the need of a feedback message. The CNN was shown to be able to provide more accurate predictions for satellites at lower orbits and for smaller distance between the uplink and downlink bands. The gated recurrent unit (GRU) architecture implemented in [6] was able to learn the temporal correlations of a LEO satellite channel based on historical time series, showing the impact of the elevation angle and the LEO altitude, among the others, on the symbol error rate. It must be mentioned that traditional algorithms have also been proposed for CSI prediction, *e.g.*, the authors in [7] implemented a closed form for the prediction of the NTN channel based on an autoregressive model of order 2 (AR(2)). However, AI-based algorithms have the potential to learn from real data and perform more accurate predictions, despite typically requiring larger computational capabilities.

In this paper, we present a low-complexity AI-based model to perform CSI prediction based on the downlink CSI feedback, the user location and the LEO satellite's ephemeris. Differently from previous works, the proposed model is trained to extract temporal statistics of not only the contributes due to the satellite's movement, but also due to correlated LoS shadowing and further additional losses that characterize NTN propagation channels. We assess the impact of the CSI prediction in a LEO-based CF-MIMO system, reporting key percentiles of the capacity achieved by each UT, as well as the outage probability.

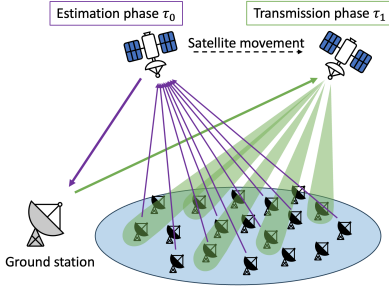


Fig. 1. System architecture.

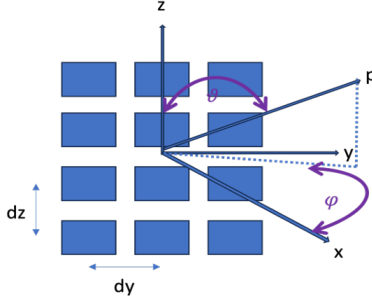


Fig. 2. UPA antenna model [8].

II. SYSTEM MODEL

In this work, we consider a LEO satellite providing connectivity from orbit to a set of UTs in a CF fashion using feed space (FS) digital beamforming (Figure 1). The satellite is equipped with an N -feed uniform planar array (UPA), represented in Figure 2, with the antenna boresight directed towards the sub-satellite point. The array response of the UPA with respect to UT i , *i.e.*, in the direction represented by the pair of angles (ϑ_i, φ_i) , can be written as:

$$\mathbf{a}(\vartheta_i, \varphi_i) = g_E(\vartheta_i, \varphi_i)(\mathbf{a}_H(\vartheta_i, \varphi_i) \otimes \mathbf{a}_V(\vartheta_i)), \quad (1)$$

where $g_E(\vartheta_i, \varphi_i)$ is the radiation pattern of an array feed, \otimes represents the Kronecker product, and $\mathbf{a}_H(\vartheta_i, \varphi_i)$ and $\mathbf{a}_V(\vartheta_i)$ are the steering vectors of two uniform linear arrays, with N_H feeds for the y axis and N_V feeds for the z axis. The two steering vectors can be computed as:

$$\mathbf{a}_H(\vartheta_i, \varphi_i) = [1, e^{jk_0 d_H \sin \vartheta_i \sin \varphi_i}, \dots, e^{jk_0 d_H (N_H - 1) \sin \vartheta_i \sin \varphi_i}] \quad (2)$$

$$\mathbf{a}_V(\vartheta_i) = [1, e^{jk_0 d_V \cos \vartheta_i}, \dots, e^{jk_0 d_V (N_V - 1) \cos \vartheta_i}] \quad (3)$$

An on-ground gNodeB (gNB), which is assumed to have continuous visibility of the satellite, performs scheduling to select a subset of K users to serve within time slot t . A coverage with a fixed N_{tier} -tiered beam pattern would allow to schedule at most one user per beam; thus, we here fix the maximum number of schedulable users per time slot to $K = 1 + 3 \times N_{\text{tier}} \times (N_{\text{tier}} + 1)$. As the scheduling algorithm is out of the scope of this paper, we here consider a random scheduler for the sake of simplicity. The gNB

transmits downlink pilot symbols at time τ_0 , which are used by the scheduled UTs to estimate the downlink FS CSI vector with respect to the N on-board feeds, $\hat{\mathbf{h}}_i$. We here consider the system level 3GPP LoS propagation model [9]:

$$\hat{\mathbf{h}}_i = \tilde{\mathbf{h}}_i^0 \times \mathbf{a}(\vartheta_i^0, \varphi_i^0), \quad (4)$$

$$\tilde{\mathbf{h}}_i^0 = G_i^{(rx)} \frac{\lambda}{4\pi d_i^0} \sqrt{\frac{L_i^0}{\kappa B T}} e^{-j \frac{2\pi}{\lambda} d_i^0}, \quad (5)$$

where $G_i^{(rx)}$ represents the i -th UT receiving gain, λ is the carrier wavelength, and d_i^0 is the slant range at time τ_0 . The CSI are normalized with respect to the noise power, represented by Boltzman's constant κ , the channel bandwidth B and the receiver noise temperature T (assumed to be the same for each UT). The term L_i^0 includes all additional losses that may incur within the i -th propagation channel at time τ_0 , *e.g.*, atmospheric attenuation L_{atm} , scintillation losses L_{scint} , and LoS shadowing L_{sh} (*e.g.*, due to foliage). In general, each contribution to the additional losses is characterized by different statistics. The atmospheric attenuation in NTN represents gaseous absorption and is thus dependent on the density and type of gas molecules encountered during propagation. Similarly, scintillation losses are also linked to physical interactions between the radiated electromagnetic wave and the gas molecules in the atmosphere, in particular in the troposphere for transmissions at a carrier frequency above 6 GHz [9]. For these two contributes, the considered channel model associates empirical constant attenuation values to different ranges of elevation angles, as these type of losses vary slowly with the satellite movement. On the other hand, LoS shadowing is modeled as a log-normal zero-mean random variable with an elevation-angle-varying standard deviation. However, each sample is typically uncorrelated from another; hence, the temporal correlation of time-consecutive shadowing samples would not be represented in this model, making it not suitable to generate time series. To take the temporal correlation into account, we assume that each shadowing sample exhibits a correlation ρ with respect to its antecedent. Hence, we represent the shadowing time series experienced by each link as an autoregressive model of order 1 (AR(1)), *i.e.*,

$$\Lambda^t = \rho \times \Lambda^{t-1} + \epsilon^t, \quad (6)$$

where ϵ^t is the realization of a zero-mean Gaussian random process with variance $\sigma_\epsilon^2 = 1 - \rho^2$, such that the generated process Λ has unit variance. The covariance of the process can then be written as $[\Sigma]_{i,j} = \rho^{|i-j|}$ [10], and the unit-variance shadowing time series can be obtained by sampling a zero-mean multivariate normal distribution with covariance matrix Σ . Finally, we obtain the length- ν shadowing time series for UT i $\{L_{\text{sh}i}\}_{1,\dots,\nu}$ by multiplying each shadowing sample in the unit-variance sequence by the shadowing standard deviation specified in the system level 3GPP model, according to the corresponding elevation angle.

After the CSI vectors are reported to the ground station, the FS beamforming matrix can be computed and used to transmit user data with space division multiplexing at time $\tau_1 = \tau_0 +$

$\Delta\tau$. $\Delta\tau$ represents the delay between the channel estimation phase and the actual data transmission:

$$\Delta\tau = \tau_{UT,max} + 2\tau_{feeder} + \tau_p + \tau_{ad}, \quad (7)$$

with $\tau_{UT,max}$ being the maximum delay between the set of scheduled UTs and the satellite, τ_{feeder} represents the delay contribution on the feeder link, τ_p including all processing delays and τ_{ad} representing possible additional losses. Clearly, as $\Delta\tau$ increases, the distance traveled by the satellite during such time interval makes the channel aging effect stronger, making the beamformed transmissions less accurate. Hence, in our proposed method, the AI-based channel prediction block is employed to project the outdated CSI amplitude $|\tilde{h}_i^0|$ to transmission time τ_1 :

$$\tilde{h}_i^{AI} = f(|\tilde{h}_i^0|, d_i^1, \alpha_i^1, \Theta) \times e^{-j\frac{2\pi}{\lambda}d_i^1}, \quad (8)$$

where d_i^1 and α_i^1 are the slant range and the elevation angle, respectively, at transmission time, and $f(\cdot)$ is a properly trained AI function with optimal parameters Θ . Assuming no user mobility, d_i^1 and α_i^1 are geometric terms that can be estimated on the network side from the position of UT i and the satellite ephemeris. It must be noted that, if user mobility was to be taken into account, the message carrying the CSI feedback should also include the UT position. As in Equation 4, the CSI vector \mathbf{h}_i^{AI} can be obtained by evaluating the UPA array response in the updated UT i direction $(\vartheta_i^1, \varphi_i^1)$. At transmission time, the K CSI vectors, either estimated at τ_0 or predicted, are collected in a $K \times N$ complex CSI matrix \mathbf{H} . The gNB then computes the complex $N \times K$ beamforming matrix \mathbf{W} using the selected beamforming algorithm. Such matrix is applied to the K user symbols to project them onto the feed space, resulting in the formation of a dedicated beam towards each scheduled UT. After propagation, the signal received by UT i can be written as [11]:

$$y_i = \mathbf{h}_i^1 \mathbf{w}_i s_i + \sum_{\substack{k=1 \\ k \neq i}}^K \mathbf{h}_i^1 \mathbf{w}_k s_k + z_i, \quad (9)$$

where $\mathbf{s} = [s_1, s_2, \dots, s_K]^T$ is the vector of user symbols to be transmitted, \mathbf{w}_i represents the beamformer dedicated to UT i (*i.e.*, the i -th column of \mathbf{W}), \mathbf{h}_i^1 represents the i -th CSI vector at transmission time τ_1 , and z_i represents additive white gaussian noise (AWGN). Clearly, the first term of the equation represents the desired contribute, while the summation contains the co-channel interference contributes deriving from beams directed towards other UTs. From these observations, the signal-to-interference-plus-noise ratio (SINR) at UT i can be assessed as follows:

$$\text{SINR}_i = \frac{\|\mathbf{h}_i^1 \mathbf{w}_i\|^2}{1 + \sum_{\substack{k=1 \\ k \neq i}}^K \|\mathbf{h}_i^1 \mathbf{w}_k\|^2}. \quad (10)$$

The capacity achievable by UT i can then be computed as:

$$\Gamma_i = B \times \log_2(1 + \text{SINR}_i). \quad (11)$$

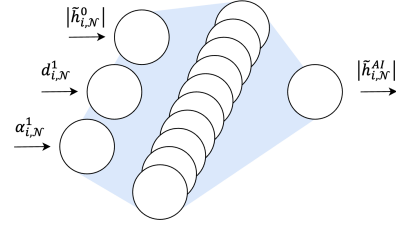


Fig. 3. AI model for CSI prediction.

Clearly, the choice of the beamforming algorithm affects the SINR, which in turn has a strong impact on the achievable user capacity. In this work, we employ the linear minimum mean squared error (MMSE) equation to compute \mathbf{W} [11]:

$$\mathbf{W} = \mathbf{H}^H (\mathbf{H}\mathbf{H}^H + \alpha_r \mathbf{I}_K)^{-1}, \quad (12)$$

where $(\cdot)^H$ is the Hermitian operator, \mathbf{I}_K is the $K \times K$ identity matrix, and α_r is the regularisation factor, here set to 1. The beamforming matrix requires a normalization step to ensure that the payload power constraints are not broken [12]. In particular, the maximum power constraint (MPC) normalization is here employed to limit the power supplied to each feed to the most stringent feed power constraint:

$$\tilde{\mathbf{W}} = \frac{\sqrt{P_{tot}} \mathbf{W}}{\sqrt{N_F \max_j [\mathbf{W}\mathbf{W}^H]_{j,j}}}. \quad (13)$$

While this power normalization maintains the column-wise orthogonality and ensures that all power constraints are respected, the limitation to the same power level results in the total available payload power not being fully utilized.

III. AI-BASED CHANNEL PREDICTION

As highlighted in the previous section, the delay $\Delta\tau$ between channel estimation and data transmission results in a mismatch between the estimated CSI matrix \mathbf{H}^0 , which is used in Equation 12 to compute the beamforming matrix, and the CSI matrix that is encountered at transmission time \mathbf{H}^1 . In particular, considering Equation 4, two main sources of mismatch can be identified:

- The variation of the slant range d_i , which affects both the amplitude and the phase of the CSI;
- The losses L_i , which affect the CSI amplitude only.

Given the satellite position, which can be obtained from ephemeris data, and the UTs positions, which are here assumed to be constant and known at the network side, the gNB can estimate the slant range for each scheduled UT. Indeed, the literature has shown that similar techniques can be employed to perform MIMO beamforming without the need of a CSI feedback from the UTs, *e.g.*, [12]. Furthermore, it must be noted that eventual phase mismatches due to imperfect slant range estimations do not affect the SINR, as the complex scalar term is canceled by the norm operator in Equation 10. However, a CSI feedback is necessary to assess the additional propagation losses. As mentioned in the previous section, each

TABLE I
SIMULATION PARAMETERS.

Parameter	Value
Carrier frequency	20 GHz
System band	Ka (400 MHz)
Receiver type	VSAT
Receiver antenna gain	39.7 dBi
Noise figure	1.2 dB
System scenario	Sub-urban
Available power per beam	2.21 dB
Number of tiers N_{tier}	{2, 4}
User density	0.05 users/km ²
Total delay $\Delta\tau$	20 ms
Number of transmitters N_F	1024 (32 × 32 UPA)

contribute to L_i exhibits a different temporal statistic, which can be learnt and partially compensated by a deep learning algorithm. We consider a fully-connected deep neural network (FC-DNN) with a single hidden layer, taking as input the amplitude of the i -th CSI at estimation time at the output of the UPA $|\tilde{h}_i^0|$, and the slant range d_i^1 and elevation angle α_i^1 experienced by UT i at transmission time τ_1 . The model is depicted in Figure 3. The input data, originated from a synthetic dataset, is standardized using the first and second order statistics of each input estimated over the entire dataset, obtaining the input vector $\mathbf{x}_N = [|\tilde{h}_{i,N}^0|, d_{i,N}^1, \alpha_{i,N}^1]$, where the subscript N indicates the data standardization. The hidden layer, composed by $N_H = 10$ fully-connected neurons, extracts optimal features from the inputs as follows:

$$\mathbf{y}_H = \mathbf{W}_H \mathbf{x}_N + \mathbf{b}_H, \quad (14)$$

where \mathbf{x}_N represents the model's input vector, and \mathbf{W}_H and \mathbf{b}_H are the weights matrix and bias vector obtained through the training process. The features are then fed to a batch normalization (BN) layer, which task is to estimate mean and standard deviation of \mathbf{y}_H during each training mini-batch and standardize the features. To introduce non-linearities in the network, the standardized features are processed through a leaky rectified linear unit (LeakyReLU) layer, which applies the following operation on each standardized feature:

$$LeakyReLU(x) = \begin{cases} x & \text{if } x > 0 \\ 0.3 \times x & \text{otherwise} \end{cases} \quad (15)$$

Finally, the activated features are combined together in a single dense output neuron \mathbf{y}_O with weights vector \mathbf{w}_O and bias b_O , representing the (standardized) predicted CSI amplitude at transmission time τ_1 . Assuming that the CSI amplitude has mean value μ_{CSI} and standard deviation σ_{CSI} over the training dataset, the predicted CSI amplitude of the i -th link has the following overall formulation:

$$\tilde{h}_i^{AI} = \tilde{h}_{i,N}^{AI} \times \sigma_{CSI} + \mu_{CSI}, \quad (16)$$

$$\tilde{h}_{i,N}^{AI} = \mathbf{w}_O \times LeakyReLU(BN(\mathbf{W}_H \mathbf{x} + \mathbf{b}_H)) + b_O. \quad (17)$$

TABLE II
AI-PREDICTED AND FEEDBACK CSI AMPLITUDE ERROR.

Method	Mean Error	Error Standard Deviation
AI-predicted CSI	0.00 dB	2.16 dB
Feedback CSI	0.00 dB	2.49 dB

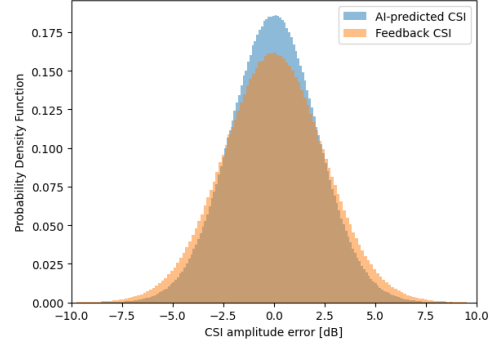


Fig. 4. Distribution of the CSI amplitude error at τ_1 .

IV. SIMULATIONS AND RESULTS

In the following section, we report the results of numerical simulations assessing the impact of the CSI prediction module on CF-MIMO systems. The FC-DNN was implemented using Python's TensorFlow library [13] and trained for 100 epochs using the popular Adam optimizer, aiming at minimizing the mean squared error (MSE) between the predicted CSI and its true value. The training, validation, and test datasets were synthetically generated using the parameters reported in Table I, based on [9], [14]. We assume that UTs can be scheduled for an integer number of consecutive 5G new radio (NR) frames of length 10 ms, and that pilot symbols for channel estimation are transmitted at the beginning of each frame. Considering Equation 7, the total delay for a LEO system can be assumed to be 16.7 ms [1]; hence, we set the total delay equal to the duration of two frames, *i.e.*, $\Delta\tau = 20$ ms.

Figure 4 reports the distribution of the CSI amplitude error on the test dataset, encompassing more than 4 million tests, for both the feedback CSI and the predicted CSI. The plot shows that the FC-DNN is able to reduce the standard deviation of the CSI amplitude error: indeed, as reported in Table II, this value decreases from 2.49 dB to 2.16 dB using the CSI prediction module. The mean error remains at 0 dB for both solutions, as expected. However, further analysis is needed to assess the impact of the AI model on the CF-MIMO performance.

To this aim, we carried out system level numerical simulations of a LEO-based CF-MIMO system on MATLAB, evaluating the capacity achieved by the UTs using Equation 11. We report in Figure 5 the 10, 50, and 90%-iles of the achieved user capacity. Regardless of N_{tier} , the AI model is able to greatly improve the capacity low 10%-iles, increasing the capacity achieved by users with low SINR. In particular, the CSI prediction increases the achievable capacity from 107 Mbps to 119 Mbps in a 2-tiered system (an 11% improvement) and from 78 Mbps to 90 Mbps in a 4-tiered system (a 15%

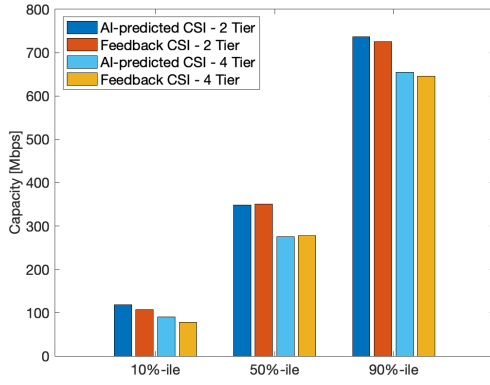


Fig. 5. Comparison of the user capacity percentiles.

improvement). UTs with large SINR also experience a slight increase in capacity (90%-ile), corresponding to 1.55% and 1.52% in systems with 2 and 4 tiers, respectively. On the opposite, the median capacity is reduced from 351 Mbps to 349 Mbps in the 4-tiered system and from 278 Mbps to 275 Mbps in the 2-tiered system. However, given the magnitude of the reduction, these last results may be within margin of error. Finally, the AI channel predictions result in lower outage probabilities, *i.e.*, the probability that the SINR falls under a minimum threshold (here set to -10 dB), from 3.02% to 1.53% with 2 tiers and from 5.47% to 3.22% with 4 tiers.

It is clear that the AI-based channel prediction module introduces an advantage within the CF-MIMO system while requiring only a fractional increase in computational complexity. Indeed, the AI model employs only 91 parameters to predict the CSI amplitude, making it extremely lightweight. Furthermore, the prediction can be carried out for multiple UTs in a single batch, exploiting the parallelization capabilities of AI techniques. It must be mentioned that, while this work is based on a synthetic dataset, real data would be necessary to ensure that the AI model is able to cope with the real additional losses statistics. Moreover, a real implementation of the proposed technique may benefit from online learning, *i.e.*, continuously or periodically fine tuning the model using recent data. Indeed, while offline learning makes the model learn general short-term statistics, online learning allows the training process to learn and take into account local variations, *e.g.*, temporary fades due to clouds or rain. Nonetheless, this work showed that the AI model is able to learn NTN channel statistics, resulting in performance gains in LEO-based CF-MIMO systems over the simple CSI feedback.

V. CONCLUSION

In this work we presented a lightweight AI model that refines outdated CSI estimates by learning and applying NTN channel statistics, projecting the CSI estimates to transmission time. We evaluated at system level the performance impact of the model on a LEO-based CF-MIMO system. Numerical analyses proved that CSI prediction enables an improvement of the user capacity 10%-iles by up to 15% and a reduction of the outage probability, regardless of the number of tiers of the

multi-beam satellite. Future works should aim at validating the AI model performance on real data, also providing a comparison in terms of accuracy and complexity with other AI-based techniques. Further activities may also assess the performance impact of CSI prediction on user scheduling.

ACKNOWLEDGMENT

This work has been funded by the 6G-NTN project, which received funding from the Smart Networks and Services Joint Undertaking (SNS JU) under the European Union's Horizon Europe research and innovation programme under Grant Agreement No 101096479. The views expressed are those of the authors and do not necessarily represent the project. The Commission is not liable for any use that may be made of any of the information contained therein.

REFERENCES

- [1] A. Guidotti, A. Vanelli-Coralli and C. Amatetti, "Federated Cell-Free MIMO in Non-Terrestrial Networks: Architectures and Performance," in *IEEE Transactions on Aerospace and Electronic Systems*, doi: 10.1109/TAES.2024.3362769.
- [2] Starlink, "SpaceX sends first test messages via its newly launched direct to cell satellites", available at: https://api.starlink.com/public-files/DIRECT_TO_CELL_FIRST_TEXT_UPDATE.pdf (accessed April 2024)
- [3] F. Riera-Palou, G. Femenias, M. Caus, M. Shaat and A. I. Pérez-Neira, "Scalable Cell-Free Massive MIMO Networks With LEO Satellite Support," in *IEEE Access*, vol. 10, pp. 37557-37571, 2022, doi: 10.1109/ACCESS.2022.3164097.
- [4] Y. Zhang, Y. Wu, A. Liu, X. Xia, T. Pan and X. Liu, "Deep Learning-Based Channel Prediction for LEO Satellite Massive MIMO Communication System," in *IEEE Wireless Communications Letters*, vol. 10, no. 8, pp. 1835-1839, Aug. 2021, doi: 10.1109/LWC.2021.3083267.
- [5] Y. Zhang, A. Liu, P. Li and S. Jiang, "Deep Learning (DL)-Based Channel Prediction and Hybrid Beamforming for LEO Satellite Massive MIMO System," in *IEEE Internet of Things Journal*, vol. 9, no. 23, pp. 23705-23715, 1 Dec.1, 2022, doi: 10.1109/JIOT.2022.3190412
- [6] G. -Y. Chang, C. -K. Hung and C. -H. Chen, "A CSI Prediction Scheme for Satellite-Terrestrial Networks," in *IEEE Internet of Things Journal*, vol. 10, no. 9, pp. 7774-7785, 1 May1, 2023, doi: 10.1109/JIOT.2022.3229683.
- [7] M. Ying and X. Chen, "Channel Prediction-based Robust Multibeam Precoding Design for LEO Satellite Internet of Things," *2023 IEEE/CIC International Conference on Communications in China (ICCC)*, Dalian, China, 2023, pp. 1-6, doi: 10.1109/ICCC57788.2023.10233532.
- [8] ITU-R Radiocommunication Sector of ITU, "Modelling and simulation of IMT networks and systems for use in sharing and compatibility studies (M.2101-0)", Feb. 2017.
- [9] 3GPP, "TR 38.811 - Study on New Radio (NR) to support non-terrestrial networks (Release 15)", Sep. 2020.
- [10] H. Kasasbeh, R. Viswanathan and L. Cao, "Noise Correlation Effect on Detection: Signals in Equicorrelated or Autoregressive(1) Gaussian," in *IEEE Signal Processing Letters*, vol. 24, no. 7, pp. 1078-1082, July 2017, doi: 10.1109/LSP.2017.2702004.
- [11] B. Ahmad, D. G. Riviello, B. De Filippo, A. Guidotti and A. Vanelli-Coralli, "Analysis of Graph-based User Scheduling for Ka-band LEO NTN Systems," *28th Ka and Broadband Communications Conference (Ka) and the 40th International Communications Satellite Systems Conference (ICSSC)*, Bradford, United Kingdom, 2023.
- [12] A. Guidotti, C. Amatetti, F. Arnal, B. Chamailard and A. Vanelli-Coralli, "Location-assisted precoding in 5G LEO systems: architectures and performances," *2022 Joint European Conference on Networks and Communications and 6G Summit (EuCNC/6G Summit)*, 2022, pp. 154-159, doi: 10.1109/EuCNC/6GSummit54941.2022.9815611.
- [13] M. Abadi et al, "TensorFlow: Large-scale machine learning on heterogeneous systems", 2015. Software available from tensorflow.org.
- [14] 3GPP, "TR 38.821 - Solutions for NR to support non-terrestrial networks (NTN)", May 2021.